Evaluating the Effect of the Second Invariant of Deformation Tensor in The Axial and Azimuthal Shear Deformations

Amir Ghafouri Sayyad, Ali Imam*, Shahram Etemadi Haghighi

Department of Mechanical Engineering, Science and Research Branch, Islamic Azad University, Tehran, Iran
E-mail: amir.ghafouriii@gmail.com, aimam@srbiau.ac.ir, setemadi@srbiau.ac.ir
*Corresponding author

Received: 19 April 2021, Revised: 9 August 2021, Accepted: 14 August 2021

Abstract: The purpose of the present paper is to investigate the effect of the second invariant of the deformation tensor on the axial and azimuthal shear deformation of an incompressible hyperelastic solid with various strain energy functions. To this end, the axial shear deformation of an incompressible cylinder with the modified Gent-Thomas, Gent-Thomas, Gent-Gent, and Carroll strain energies subjected to an axial shear traction is considered, where the displacement field is determined analytically for the first three models and numerically for the fourth model. The phenomenon of strain hardening at large elastic deformations, predicted either by the limiting chain extensibility condition for the modified Gent-Thomas and Gent-Gent models or phenomenologically by the Carroll model, is observed and it is shown that the second invariant of deformation increases the strain hardening experienced by such materials. Next, the azimuthal shear deformation of an incompressible annular wedge with the modified Gent-Thomas, Gent-Thomas, Gent-Gent, and Carroll models is considered, where the annular wedge is subjected to a controllable azimuthal shear deformation and the angular displacement is determined analytically for all the above models. Again, the second invariant of the deformation tensor is shown to have a significant effect on the azimuthal shear deformation as reflected in the increase of the strain hardening of the material in such deformation. In addition, the annular wedge with the modified Gent-Thomas and Carroll models is shown to have a higher resistance in azimuthal shear deformation than the other models mentioned above.

Keywords: Axial Shear, Azimuthal Shear, Strain Hardening, Controllable Deformation, Incompressible Hyperelastic Solids, Second Invariant of the Deformation Tensor

How to cite this paper: Amir Ghafouri Sayyad, Ali Imam, and Shahram Etemadi Haghighi, "Evaluating the Effect of the Second Invariant of Deformation Tensor in The Axial and Azimuthal Shear Deformations", Int J of Advanced Design and Manufacturing Technology, Vol. 15/No. 1, 2022, pp. 95–107
DOI: 10.30495/admt.2021.1928399.1275.

Biographical notes: Amir Ghafouri Sayyad received his MSc in Mechanical Engineering from the Islamic Azad University of Takestan in 2010. At present, he is a PhD student of the IAU university, science and research branch of Tehran. **Ali Imam** is an assistant professor of Mechanical Engineering at IAU university, science and research branch of Tehran, Iran. He received his PhD in Mechanical Engineering from University of California in 1993. His current research focuses on continuum mechanics and non-linear elasticity. **Shahram Etemadi Haghighi** is an assistant professor of Mechanical Engineering at IAU university, science and research branch of Tehran, Iran. He received his PhD in Mechanical Engineering from Sharif University of Technology, Tehran, Iran in 2011. His current research subjects are nonlinear systems and dynamics.

1 INTRODUCTION

There are various models for hyperelastic materials whose elastic response is determined based on a strain energy function. If the material is isotropic and incompressible, the strain energy function depends on the first and second invariant of the deformation tensor with the third invariant, in this case, being equal to one. Although the elastic response of the materials whose strain energy function depends only on the first invariant has been studied quite extensively, the effect of the second invariant on the elastic response of the materials whose strain energy depends on both invariants has been less studied. This is partly because the analysis of the deformation field when the second invariant is present is often more complicated which makes finding analytical solutions less likely.

Among the strain energy functions, the Mooney-Rivlin model is one of the simplest hyperelastic models for incompressible solids. Another model known as the Gent-Thomas model has also been able to meet the experimental requirements rather well. This model is suitable for continuous and bulk material analysis [1] and models the response of vulcanized and porous rubber better than the Mooney-Rivlin model [2-3].

In the present paper, the effect of the second invariant of the deformation tensor on the axial and azimuthal shear deformation for several strain energy models is studied. The strain energy models include the Gent-Thomas [4], modified Gent-Thomas, Gent-Gent [5], and Carroll models [6]. The modified Gent-Thomas model, first proposed by Gent [7], and the Gent-Gent model also known as the Pucci-Saccomandi model [5], incorporate the limiting chain extensibility parameter to model the molecular polymeric behaviour of rubber-like materials. This parameter is partly the cause of work or strain hardening of the material at large deformations observed at the macroscopic level. Other various models such as the Gent [8], Van der Waals [9], and Edward Vilgis [10] also incorporate the limiting chain extensibility parameter but are not considered here since the strain hardening effect is well represented by the four models mentioned above. The Carroll model, being a phenomenological model and not based on the microstructure, also predicts the strain hardening phenomenon.

In the first part of the present paper, a circular cylinder undergoing axial shear deformation is considered. In the context of this type of deformation, quite a large number of studies have been performed so far. Due to the extent of such studies, only a few ones more relevant to the present study are mentioned here. In such studies, deformation of a circular cylindrical tube is considered with the assumption of a fixed internal boundary which is subjected to a uniformly distributed axial shear traction on the external boundary under various hypotheses. Such hypotheses include combined shearing deformation of a prestressed tube (torsion, azimuthal, and axial shear) [11], combined axial and azimuthal shear deformation of an incompressible [12] and a compressible material [13], deformation of a rubber material with strain stiffening[14], deformation of a material having strain energy with limiting chain extensibility condition [15], motion of an elastic solid having generalized neo-Hookean strain energy exposed to a periodic shear on the inner boundary [16], and deformation of materials that undergo strain hardening [17].

In a study by Carroll, a new strain energy function for an incompressible material having three parameters, based on the behaviour of vulcanized rubber, was proposed [6]. In this study, the new model was developed based on the Treloar, Rivlin-Saunders, and Jones's experiments on sheets of vulcanized rubber, with remarkable capability for predicting the behaviour of rubber-like materials over a wide range of deformations [18-19]. As mentioned before, the Carroll model, being a phenomenological model, predicts the strain hardening phenomenon from a macroscopic viewpoint.

In the context of azimuthal shear deformation, many studies have been carried out. Such investigations include the study of a circular cylindrical tube with the assumption of a fixed internal boundary and subjected to a uniformly distributed azimuthal shear traction on the external boundary, in which various hypotheses are made. Such hypotheses include compressibility [20], large shearing (extension, inflation, torsion, and helical shear) in a prestressed tube [21], limiting chain extensibility condition [22], and reinforcement by radial fibers [23]. Also, some universal solutions for isotropic and incompressible materials subjected to different types of deformation such as azimuthal shear of an annular wedge [24] have been investigated.

El Hamdaoui, Merodio, and Ogden [25] have analyzed the ellipticity condition in an isotropic tube that is subjected to a combined deformation such as axial extension with axial and azimuthal shear wherein basic equations were derived and loss of ellipticity was examined.

In addition, combined deformation, such as the helical shear (azimuthal and axial shear) of a hardening generalized neo-Hookean elastic material was investigated by Horgan and Saccomandi [26]. In their study, the components of stress and angular and axial displacements are determined and compared with the corresponding ones for the classical neo-Hookean model.

It is noteworthy that in most of the above studies, the strain energies that were considered depend only on the first invariant of the deformation tensor, whereas the strain energy models considered in the present paper depend on both the first and second invariants of the

deformation tensor. The importance of including the second invariant of the deformation tensor in the strain energy function is also discussed by Anssari-Benam and Bucchni in [27].

In the present paper, the effect of the second invariant of the deformation tensor on the strain hardening of incompressible materials with various strain energy models in the axial and azimuthal shear deformation is compared. Such models include the modified Gent-Thomas, Carroll, Gent-Gent, and Gent-Thomas models. This comparison has not been reported before and provides additional insight into the role of the second invariant in the deformation of hyperelastic materials. In addition, the axial and azimuthal shear deformations considered in this study are nonhomogeneous deformations for which the effect of the second invariant on the deformation of hyperelastic materials with the above strain energy models has yet to be investigated.

In Section 2 of the present paper, analysis of the axial shear deformation for several models is carried out whereby integration of the equations of equilibrium yields the axial displacement field in quadrature form, i.e., in the form of an integral. In Section 3, analysis of a controllable azimuthal shear deformation for several models is carried out. The use of controllable azimuthal shear deformation makes it possible to obtain an analytical solution for the stress field. The general azimuthal shear deformation is treated in Ghafouri et. al. [28] in which it may not be possible in general to obtain analytical solutions.

The results obtained for the axial and azimuthal shear deformation for various models are discussed and compared in detail in Section 4. Finally, in Section 5, some conclusions are drawn with respect to the effect of the second invariant of the deformation tensor on the response of an incompressible isotropic hyperelastic solid in axial and azimuthal shear deformations.

2 AXIAL SHEAR DEFORMATION

It is assumed that an incompressible hyperelastic isotropic cylinder is undergoing the deformation [29]:

$$r = R \quad , \quad \theta = \Theta \quad , \quad z = Z + f(R) \tag{1}$$

Where, (R, Θ, Z) and (r, θ, z) are the cylindrical coordinates in the reference and spatial configurations, respectively, with $R_1 \le R \le R_2$, where R_1 and R_2 denote the inner and outer radii, respectively. In this deformation, a material point undergoes axial shear with dependence on the radial direction. In addition, the inner boundary of the cylinder is held fixed, i.e., $f(r=r_1)=0$, and its outer boundary is acted upon by a uniformly distributed axial shear traction, $t_{rz}(r=r_2)=T_1$, while the other tractions, t_{rr} and $t_{r\theta}$, at the outer boundary are zero. The deformation gradient tensor **F**, the left Cauchy-Green deformation tensor **B**, and its inverse $\mathbf{B}^{-1}$ for this deformation are, respectively:

$$\mathbf{F} = \begin{pmatrix} 1 & 0 & 0 \\ 0 & 1 & 0 \\ f' & 0 & 1 \end{pmatrix}, \mathbf{B} = \begin{pmatrix} 1 & 0 & f' \\ 0 & 1 & 0 \\ f' & 0 & 1+f'^2 \end{pmatrix}, \quad \mathbf{B}^{-1} = \begin{pmatrix} 1+f'^2 & 0 & -f' \\ 0 & 1 & 0 \\ -f' & 0 & 1 \end{pmatrix} \tag{2}$$

Where, $f' = \mathrm{d}f/\mathrm{d}R = \mathrm{d}f/\mathrm{d}r$. Incompressibility condition for this deformation holds since $\det \mathbf{F}=1$.

The principal invariants of **B** are:

$$I_1 = \mathrm{tr}\,\mathbf{B} = 3 + f'^2, \; I_2 = \mathrm{tr}\,\mathbf{B}^{-1} = 3 + f'^2, \; I_3 = \det \mathbf{B} = 1 \tag{3}$$

Using the Cayley-Hamilton theorem for an isotropic, incompressible material, the stress tensor is given by:

$$\mathbf{T} = -p\,\mathbf{I} + \beta_1 \mathbf{B} + \beta_{-1}\mathbf{B}^{-1} \tag{4}$$

Where, β_1 and β_{-1} are material parameters are defined as [30]:

$$\beta_1 = 2(I_3)^{-\frac{1}{2}} \frac{\partial W}{\partial I_1}, \; \beta_{-1} = -2(I_3)^{\frac{1}{2}} \frac{\partial W}{\partial I_2} \tag{5}$$

Therefore, the components of stress for the hyperelastic material are:

$$t_{rr} = -p + \beta_1 + \beta_{-1}(1 + f'^2) \tag{6}$$

$$t_{\theta\theta} = -p + \beta_1 + \beta_{-1} \tag{7}$$

$$t_{zz} = -p + \beta_1(1 + f'^2) + \beta_{-1} \tag{8}$$

$$t_{rz} = (\beta_1 - \beta_{-1}) f' \tag{9}$$

$$t_{r\theta} = t_{z\theta} = 0 \tag{10}$$

In the above relations, p is a hydrostatic pressure resulting from material incompressibility, which can be determined using the equilibrium equations and the boundary conditions.

For later reference, the equilibrium equations in cylindrical coordinates, in the absence of body forces, are recorded below.

$$\frac{\partial t_{rr}}{\partial r}+\frac{1}{r}\frac{\partial t_{r\theta}}{\partial \theta}+\frac{\partial t_{rz}}{\partial z}+\frac{1}{r}(t_{rr}-t_{\theta\theta})=0 \tag{11}$$

$$\frac{\partial t_{r\theta}}{\partial r}+\frac{1}{r}\frac{\partial t_{\theta\theta}}{\partial \theta}+\frac{\partial t_{\theta z}}{\partial z}+\frac{2}{r}(t_{r\theta})=0 \tag{12}$$

$$\frac{\partial t_{rz}}{\partial r}+\frac{1}{r}\frac{\partial t_{\theta z}}{\partial \theta}+\frac{\partial t_{zz}}{\partial z}+\frac{1}{r}(t_{rz})=0 \tag{13}$$

In what follows, the stress field is used to determine the axial force and axial displacement in the axial shear deformation for several strain energy models.
The hydrostatic pressure can be determined using "Eqs. (6) and (11)" as:

$$p(r)=(\beta_1+\beta_{-1}(1+f'^2))+\int_r^{r_2}\frac{1}{r}(\beta_{-1}f'^2)dr \tag{14}$$

Finally, the axial force N', needed to maintain the deformation, is determined by the relation:

$$N'=\int_0^{2\pi}\int_{r_1}^{r_2} t_{zz}\,r\,\mathrm{d}r\,\mathrm{d}\theta=2\pi\int_{r_1}^{r_2} t_{zz}\,r\,\mathrm{d}r \tag{15}$$

2.1. Gent-Thomas Model

Gent and Thomas [4] proposed the following strain energy function for an incompressible material:

$$W_{GT}=K_1(I_1-3)+K_2\ln(\frac{I_2}{3}) \tag{16}$$

Where, K_1 and K_2 are material parameters obtained from Kawabata's experiments (biaxial tensile) [31]. These parameters are given in "Table 1".

Table 1 The Gent-Thomas material parameters using Kawabata experimental data [29]

Parameters	N/mm^2
K_1	0.153
K_2	0.147

For the Gent-Thomas model defined in "Eq. (16)", the components of stress are found using "Eq. (3), Eqs. (5-10)" as:

$$t_{rr}=-p+2K_1-\frac{2K_2}{3+f'^2}(1+f'^2) \tag{17}$$

$$t_{\theta\theta}=-p+2K_1-\frac{2K_2}{3+f'^2} \tag{18}$$

$$t_{zz}=-p+2K_1(1+f'^2)-\frac{2K_2}{3+f'^2} \tag{19}$$

$$t_{rz}=2(K_1+\frac{K_2}{3+f'^2})f' \tag{20}$$

$$t_{r\theta}=t_{z\theta}=0 \tag{21}$$

The shearing stress t_{rz} is determined using "Eq. (13)" and the boundary condition $t_{rz}(r=r_2)=T_1$ to be:

$$t_{rz}=\frac{T_1 r_2}{r} \tag{22}$$

Next, an equation for the axial shear function f is obtained using "Eqs. (20) and (22)", which may be written as:

$$f'^3-\frac{\alpha}{r}f'^2+K\,f'-\frac{3\alpha}{r}=0 \tag{23}$$

Where $\alpha=T_1 r_2/2K_1$ and $K=(3K_1+K_2)/K_1$.
Equation (23) has three roots, two of which are complex conjugates and therefore not physically acceptable. The only real root is found to be:

$$f'=\frac{\alpha}{3r}+\left(\sqrt{A^2+C^3}+A\right)^{\frac{1}{3}}+\frac{-\left(\frac{\alpha^2}{9r^2}-\frac{K}{3}\right)}{\left(\sqrt{A^2+C^3}+A\right)^{\frac{1}{3}}} \tag{24}$$

Where:

$$A=\frac{\alpha^3}{27r^3}+\frac{3\alpha}{2r}-\frac{\alpha K}{6r} \tag{25}$$

$$C=\frac{K}{3}-\frac{\alpha^2}{9r^2} \tag{26}$$

Equation (24) is rewritten using the dimensionless parameter $T=T_1/K_1$ as:

$$f'=\frac{\alpha}{3r}+\left(\sqrt{\bar{A}^2+\bar{C}^3}+\bar{A}\right)^{\frac{1}{3}}+\frac{-\left(\frac{\alpha^2}{9r^2}-\frac{K}{3}\right)}{\left(\sqrt{\bar{A}^2+\bar{C}^3}+\bar{A}\right)^{\frac{1}{3}}} \tag{27}$$

Where:

$$\bar{A} = \frac{T^3 r_2^3}{216 r^3} + \frac{3T r_2}{4r} - \frac{T r_2 K}{12 r^2} \tag{28}$$

$$\bar{C} = \frac{K}{3} - \frac{T^2 r_2^2}{36 r^2} \tag{29}$$

Finally, the hydrostatic pressure is found using "Eqs. (5), (14), and (16)", and also the axial force is found, using "Eqs. (5), (8), (16), and (15)" to be:

$$p(r) = 2K_1 - \frac{2K_2}{3+f'^2}\left(1+f'^2\right) - \int_r^{r_2} \frac{2}{r}\left(\frac{K_2}{3+f'^2} f'^2\right) dr \tag{30}$$

$$N' = 2\pi \int_{r_1}^{r_2} \left(-p + 2K_1(1+f'^2) - \frac{2K_2}{3+f'^2}\right) r \, dr \tag{31}$$

In the above equations, f' is obtained from "Eq. (24)".

2.2. Modified Gent-Thomas

The Gent-Thomas strain energy can be modified by incorporating the limiting chain extensibility condition according to [7]:

$$W_{\mathrm{MGT}} = -K_1 J_m \ln\left(1 - \frac{I_1 - 3}{J_m}\right) + K_2 \ln\left(\frac{I_2}{3}\right) \tag{32}$$

Where, J_m is a constant resulting from the limiting chain extensibility condition. As $J_m \to \infty$ in "Eq. (32)", the Gent-Thomas strain energy in "Eq. (16)" is recovered. A similar model has been proposed by Pucci and Saccomandi [5], however, the material parameters of their proposed model are different from those in "Eq. (32)".

The components of stress for the modified Gent-Thomas model, using "Eq. (3), Eqs. (5-10), Eq. (32)", and the boundary condition $t_{rr}(r=r_2) = 0$ are found to be:

$$t_{rr} = -p + \frac{2K_1}{1 - \frac{f'^2}{J_m}} - \frac{2K_2}{3+f'^2}(1+f'^2) \tag{33}$$

$$t_{\theta\theta} = -p + \frac{2K_1}{1 - \frac{f'^2}{J_m}} - \frac{2K_2}{3+f'^2} \tag{34}$$

$$t_{zz} = -p + \frac{2K_1}{1 - \frac{f'^2}{J_m}}(1+f'^2) - \frac{2K_2}{3+f'^2} \tag{35}$$

$$t_{rz} = 2\left(\frac{K_1}{1 - \frac{f'^2}{J_m}} + \frac{K_2}{3+f'^2}\right) f' \tag{36}$$

$$t_{r\theta} = t_{z\theta} = 0 \tag{37}$$

For this material, similar to the Gent-Thomas model, the shearing stress t_{rz} can be obtained from "Eq. (22)" . Therefore, the equation for the axial shear function is obtained using "Eqs. (22) and (36)" as:

$$\begin{aligned} &\frac{T_1 r_2}{2r(J_m K_1 - K_2)} f'^4 + f'^3 - \frac{T_1 r_2 (J_m - 3)}{2r(J_m K_1 - K_2)} f'^2 \\ &+ \frac{J_m (3k_1 + K_2)}{(J_m K_1 - K_2)} f' - \frac{3 J_m T_1 r_2}{2r(J_m K_1 - K_2) r} = 0 \end{aligned} \tag{38}$$

In the above equation, as $J_m \to \infty$, "Eq. (23)" is recovered. Equation (38) is rewritten using the dimensionless parameter $T = T_1/K_1$:

$$\begin{aligned} &\frac{T b}{r} f'^4 + f'^3 - \frac{T b}{r}(J_m - 3) f'^2 \\ &+ K_m J_m f' - \frac{3 T b J_m}{r} = 0 \end{aligned} \tag{39}$$

Where:

$$b = \frac{K_1 r_2}{2(K_1 J_m - K_2)}, \quad K_m = \frac{(3K_1 + K_2)}{(J_m K_1 - K_2)} \tag{40}$$

Equation (39) has four real roots only two of which have positive signs that are physically relevant so that $f'(R) > 0$. The four roots of "Eq. (39)" are recorded in the Appendix. Of the two positive roots, the second one is real in the range $0 \le T \le 4.5$ throughout the thickness of the tube, while the fourth one is imaginary throughout the thickness. In the range where $9.15 < T \le 65$, the fourth root is real and the second root is imaginary throughout the thickness of the tube. In the range where $4.5 < T \le 9.15$, the second root is real on some interval in the radial direction while the fourth root is real on the complement of that interval. For example, for $T = 5.1$, the fourth root given by "Eq. (A4)" is real only for $2 \le r \le 2.24$ while the second root given by "Eq. (A2)" is real only on the complementary interval $2.24 < r \le 4.0$. Hence, in the latter range, integration is performed using both roots on two complementary intervals in order to determine the angular displacement. The hydrostatic pressure and the axial force for this material, analogous to the Gent-Thomas model, can be determined as :

$$p(r)=2(\frac{K_1}{1-\frac{f'^2}{J_m}}-\frac{K_2}{3+f'^2}(1+f'^2)) \\ -2\int_r^{r_2}\frac{f'^2}{r}(\frac{K_1}{1-\frac{f'^2}{J_m}}+\frac{K_2}{3+f'^2})\mathrm{d}r \quad (41)$$

$$N'=2\pi\int_{r_1}^{r_2}(-p+\frac{2K_1}{1-\frac{f'^2}{J_m}}(1+f'^2)-\frac{2K_2}{3+f'^2})r\,\mathrm{d}r \quad (42)$$

Where, f' is obtained from "Eq. (39)" and the Appendix.

2.3. Pucci-Saccomandi or the Gent-Gent model

The Pucci-Sacamendi model is very similar to the modified Gent-Thomas model with the only difference being in their material parameters. The strain energy for this model, also known as the Gent-Gent model, is defined by [5]:

$$W_{GG}=-\frac{\mu}{2}J_m\ln(1-\frac{I_1-3}{J_m})+C_2\ln(\frac{I_2}{3}) \quad (43)$$

Where, J_m is the limiting chain extensibility parameter. In "Eq. (43)", J_m=88.13 and material parameters μ and C_2, obtained using Treloar's equibiaxial tension data [31], are given in "Table 2".

Table 2 The Gent-Gent material parameters [31]

Parameters	N/mm^2
μ	0.3106
C_2	0.0428

It is noted that the Gent-Gent strain energy is similar to the modified Gent-Thomas strain energy, the only difference is that the constants K_1 and K_2 in the latter model replace the constants $\mu/2$ and C_2 in the former model.

2.4. Carroll model

The phenomenon of strain hardening at large elastic deformations can be examined from both the microscopic and macroscopic points of view. From the microscopic viewpoint, the material behavior at the molecular level is constraint by the limiting chain extensibility condition causing it to develop strain hardening. Various models such as Gent, Van der Waals, and Edwards-Vilgis predict strain hardening by incorporating the limiting chain extensibility condition [8-10]. In the macroscopic viewpoint, however, strain hardening may be predicted by a phenomenological constitutive relation as embodied in the strain energy function. As an example, Carroll [6] proposed the following strain energy function for an incompressible material:

$$W_C=A_1I_1+A_2I_1^{\,4}+A_3I_2^{\frac{1}{2}} \quad (44)$$

Where, A_1, A_2, and A_3 are material parameters obtained from Treloar's equibiaxial tension tests given in "Table 3".

Table 3 The Carroll model parameters using Treloar's equibiaxial tension tests [6]

Parameters	N/mm^2
A_1	0.15
A_2	3.1×10^{-7}
A_3	0.095

The shear stress t_{rz} for this model is found using "Eqs. (2-10)", and "Eq. (44)" to be:

$$t_{rz}=(2A_1+8A_2(3+f'^2)^3+\frac{A_3}{(3+f'^2)^{\frac{1}{2}}})f' \quad (45)$$

Equation (45) is rewritten using the dimensionless parameter, $T=T_1/A_1$ as:

$$(2+8\frac{A_2}{A_1}(3+f'^2)^3+\frac{\frac{A_3}{A_1}}{(3+f'^2)^{\frac{1}{2}}})f'-\frac{Tr_2}{r}=0 \quad (46)$$

Finding an analytical solution for "Eq. (46)", having a high order, poses difficulties and therefore a numerical solution is obtained using the Mathematica software. The results are illustrated in "Figs. 1 and 2" and discussed in detail in Section 4.

The hydrostatic pressure and the axial force for this material can be calculated using "Eqs. (5), (8), (14), (15), and (44)" as:

$$p(r)=(2A_1+8A_2(3+f'^2)^3-\frac{A_3}{(3+f'^2)^{\frac{1}{2}}}(1+f'^2)) \\ -\int_r^{r_2}\frac{2}{r}(\frac{A_3}{(3+f'^2)^{\frac{1}{2}}}f'^2)\mathrm{d}r \quad (47)$$

$$N'=2\pi\int_{r_1}^{r_2}(-p+(2A_1+8A_2(3+f'^2)^3)(1+f'^2))r\,\mathrm{d}r \\ -2\pi\int_{r_1}^{r_2}\frac{A_3}{(3+f'^2)^{\frac{1}{2}}}r\,\mathrm{d}r \quad (48)$$

Where, f' is the root of "Eq. (46)".

3 AZIMUTHAL SHEAR DEFORMATION

In this Section, azimuthal shearing of an annular wedge is considered. It is assumed that an incompressible hyperelastic annular wedge is undergoing the deformation [30]:

$$r = R \ , \quad \theta = \Theta + \mathrm{g}(R) \ , \quad z = Z \tag{49}$$

Where, (R, Θ, Z) and (r, θ, z) are the cylindrical coordinates in the reference and spatial configurations, respectively, with $R_1 \le R \le R_2$, where R_1 and R_2 denote the inner and outer radii, respectively. In this deformation, a material point undergoes azimuthal shear deformation with dependence on the radial direction. In addition, the internal boundary of the annular wedge is held fixed, i.e., $g(r=r_1)=0$, and its outer boundary is acted upon by a uniformly distributed azimuthal shear traction, $t_{r\theta}(r=r_2)=T_0$. The angle of twist at the outer boundary is denoted by $g(r=r_2)=\Psi$, while the other tractions, t_{rr} and t_{rz}, at the outer boundary are zero.

In this section, a specific form of the shear deformation given in "Eq. (49)" is considered [30], namely:

$$r = R \ , \quad \theta = \Theta + D\ln(R) \ , \quad z = Z \tag{50}$$

Where, D is a constant and $\mathrm{g}(R)=D\ln(R)$. This is a controllable deformation, i.e., it can be supported in every hyperelastic incompressible isotropic material by applying the appropriate surface tractions without applying body forces. The advantage of using a controllable deformation is that the applied shear traction at the outer boundary can be found explicitly in terms of the angle of twist. However, for the general azimuthal shear deformation given in "Eq. (49)" analytical solutions for some of the strain energy models considered here are obtained in [31].

The angle of twist obtained using "Eq. (50)" is given by:

$$\Psi = g(R = R_2) = \int_{R_1}^{R_2} g' \,\mathrm{d}R \tag{51}$$

Where, $\mathrm{g}'(R)=\mathrm{g}'(r)=\mathrm{D/r}$. Thus "Eq. (50)" is used to obtain the constant D as:

$$\Psi = D\ln(\frac{r_2}{r_1}) \Rightarrow D = \frac{\Psi}{\ln(\frac{r_2}{r_1})} \tag{52}$$

The deformation gradient tensor **F**, the left Cauchy-Green deformation tensor **B**, and its inverse $\mathbf{B}^{-1}$ for this deformation are, respectively:

$$\mathbf{F} = \begin{pmatrix} 1 & 0 & 0 \\ \dfrac{\Psi}{\ln(\frac{r_2}{r_1})} & 1 & 0 \\ 0 & 0 & 1 \end{pmatrix},$$

$$\mathbf{B} = \mathbf{F}\mathbf{F}^{\mathrm{T}} = \begin{pmatrix} 1 & \dfrac{\Psi}{\ln(\frac{r_2}{r_1})} & 0 \\ \dfrac{\Psi}{\ln(\frac{r_2}{r_1})} & 1+(\dfrac{\Psi}{\ln(\frac{r_2}{r_1})})^2 & 0 \\ 0 & 0 & 1 \end{pmatrix}, \tag{53}$$

$$\mathbf{B}^{-1} = \begin{pmatrix} 1+(\dfrac{\Psi}{\ln(\frac{r_2}{r_1})})^2 & -\dfrac{\Psi}{\ln(\frac{r_2}{r_1})} & 0 \\ -\dfrac{\Psi}{\ln(\frac{r_2}{r_1})} & 1 & 0 \\ 0 & 0 & 1 \end{pmatrix}$$

Incompressibility condition for this deformation holds since $\det \mathbf{F}=1$. The principal invariants of **B** are:

$$I_1 = I_2 = 3 + (\frac{\Psi}{\ln(\frac{r_2}{r_1})})^2, \ I_3 = \det \mathrm{B} = 1 \tag{54}$$

The components of stress can be obtained using "Eqs. (4), (53), and (54)" as:

$$t_{rr} = -p + \beta_1 + \beta_{-1}(1 + (\frac{\Psi}{\ln(\frac{r_2}{r_1})})^2) \tag{55}$$

$$t_{\theta\theta} = -p + \beta_1(1 + (\frac{\Psi}{\ln(\frac{r_2}{r_1})})^2) + \beta_{-1} \tag{56}$$

$$t_{zz} = -p + \beta_1 + \beta_{-1} \tag{57}$$

$$t_{r\theta} = (\beta_1 - \beta_{-1})\frac{\Psi}{\ln(\frac{r_2}{r_1})} \tag{58}$$

$$t_{rz} = t_{\theta z} = 0 \tag{59}$$

Where, p is the hydrostatic pressure.

3.1. Gent-Thomas model

For the Gent-Thomas model defined in "Eq. (16)", the components of stress are found, using "Eqs. (5) and (55-59)", to be:

$$t_{rr} = -p + 2K_1 - \frac{2K_2}{3+\left(\frac{\Psi}{\ln\left(\frac{r_2}{r_1}\right)}\right)^2}\left(1+\left(\frac{\Psi}{\ln\left(\frac{r_2}{r_1}\right)}\right)^2\right) \tag{60}$$

$$t_{\theta\theta} = -p + 2K_1\left(1+\left(\frac{\Psi}{\ln\left(\frac{r_2}{r_1}\right)}\right)^2\right) - \frac{2K_2}{3+\left(\frac{\Psi}{\ln\left(\frac{r_2}{r_1}\right)}\right)^2} \tag{61}$$

$$t_{zz} = -p + 2K_1 - \frac{2K_2}{3+\left(\frac{\Psi}{\ln\left(\frac{r_2}{r_1}\right)}\right)^2} \tag{62}$$

$$t_{r\theta} = 2\left(K_1 + \frac{K_2}{3+\left(\frac{\Psi}{\ln\left(\frac{r_2}{r_1}\right)}\right)^2}\right)\left(\frac{\Psi}{\ln\left(\frac{r_2}{r_1}\right)}\right) \tag{63}$$

$$t_{\theta z} = t_{rz} = 0 \tag{64}$$

According to "Eq. (63)", shear stress is constant and the boundary condition is specified as $t_{r\theta}(r=r_2)=T_0$. Therefore, it follows from "Eq. 63" that:

$$2\left(\frac{\Psi}{\ln\left(\frac{r_2}{r_1}\right)}\right)\left(K_1 + \frac{K_2}{3+\left(\frac{\Psi}{\ln\left(\frac{r_2}{r_1}\right)}\right)^2}\right) = T_0 \tag{65}$$

Equation (65) is rewritten using the dimensionless parameter $\bar{T}=T_0/K_1$ as

$$\bar{T} = 2\left(\frac{\Psi}{\ln\left(\frac{r_2}{r_1}\right)}\right)\left(1+\frac{\frac{K_2}{K_1}}{3+\left(\frac{\Psi}{\ln\left(\frac{r_2}{r_1}\right)}\right)^2}\right) \tag{66}$$

3.2. Modified Gent-Thomas Model

The stress components for the modified Gent-Thomas strain energy are found, using "Eqs. (5), (32), and (55-59)", to be:

$$t_{rr} = -p + \frac{2K_1}{\left(\frac{\Psi}{\ln\left(\frac{r_2}{r_1}\right)}\right)^2}\Bigg/\left(1-\frac{r_1}{J_m}\right) - \frac{2K_2}{3+\left(\frac{\Psi}{\ln\left(\frac{r_2}{r_1}\right)}\right)^2}\left(1+\left(\frac{\Psi}{\ln\left(\frac{r_2}{r_1}\right)}\right)^2\right) \tag{67}$$

$$t_{\theta\theta} = -p + \frac{2K_1}{\left(\frac{\Psi}{\ln\left(\frac{r_2}{r_1}\right)}\right)^2}\left(1+\left(\frac{\Psi}{\ln\left(\frac{r_2}{r_1}\right)}\right)^2\right)\Bigg/\left(1-\frac{r_1}{J_m}\right) - \frac{2K_2}{3+\left(\frac{\Psi}{\ln\left(\frac{r_2}{r_1}\right)}\right)^2} \tag{68}$$

$$t_{zz} = -p + \frac{2K_1}{\left(\frac{\Psi}{\ln\left(\frac{r_2}{r_1}\right)}\right)^2}\Bigg/\left(1-\frac{r_1}{J_m}\right) - \frac{2K_2}{3+\left(\frac{\Psi}{\ln\left(\frac{r_2}{r_1}\right)}\right)^2} \tag{69}$$

$$t_{r\theta} = 2\left(\frac{K_1}{\left(\frac{\Psi}{\ln\left(\frac{r_2}{r_1}\right)}\right)^2} + \frac{K_2}{3+\left(\frac{\Psi}{\ln\left(\frac{r_2}{r_1}\right)}\right)^2}\right)\Bigg/\left(1-\frac{r_1}{J_m}\right)\left(\frac{\Psi}{\ln\left(\frac{r_2}{r_1}\right)}\right) \tag{70}$$

$$t_{\theta z} = t_{rz} = 0 \tag{71}$$

For this model, similar to the Gent-Thomas model, the applied shear traction in terms of the angle of twist can be obtained using "Eq. (70)", the outer boundary condition, and the dimensionless parameter $\bar{T}=T_0/K_1$ as;

$$\bar{T} = 2\left(\frac{1}{\left(\frac{\Psi}{\ln\left(\frac{r_2}{r_1}\right)}\right)^2} + \frac{\frac{K_2}{K_1}}{3+\left(\frac{\Psi}{\ln\left(\frac{r_2}{r_1}\right)}\right)^2}\right)\Bigg/\left(1-\frac{r_1}{J_m}\right)\left(\frac{\Psi}{\ln\left(\frac{r_2}{r_1}\right)}\right) \tag{72}$$

The angular displacement equation for the Gent-Gent strain energy is similar to that of the modified Gent-

Thomas strain energy, the only difference being that the constants K_1 and K_2 in the latter model replace the constants $\mu/2$ and C_2 in the former model.

3.3. Carroll Model

Analogous to the above-mentioned models, the shear stress $t_{r\theta}$, for this model is found, using "Eqs. (5), (44), and (55-59)", to be:

$$t_{r\theta} = (2A_1 + 8A_2(3+(\frac{\Psi}{\ln(\frac{r_2}{r_1})})^2)^3(\frac{\Psi}{\ln(\frac{r_2}{r_1})}) + \frac{A_3}{(3+(\frac{\Psi}{\ln(\frac{r_2}{r_1})})^2)^{\frac{1}{2}}})(\frac{\Psi}{\ln(\frac{r_2}{r_1})}) \quad (73)$$

The applied shear traction in terms of the angle of twist for this model can be obtained, using "Eq. (73)" and the outer boundary condition, as:

$$(2A_1 + 8A_2(3+(\frac{\Psi}{\ln(\frac{r_2}{r_1})})^2)^3)(\frac{\Psi}{\ln(\frac{r_2}{r_1})})^2 + \frac{A_3}{(3+(\frac{\Psi}{\ln(\frac{r_2}{r_1})})^2)^{\frac{1}{2}}})(\frac{\Psi}{\ln(\frac{r_2}{r_1})})^2 - T_0 = 0 \quad (74)$$

Equation (74) is rewritten using the dimensionless parameter $\bar{T}=T_0/A_1$ as:

$$\bar{T} = (2+8\frac{A_2}{A_1}(3+(\frac{\Psi}{\ln(\frac{r_2}{r_1})})^2)^3)(\frac{\Psi}{\ln(\frac{r_2}{r_1})}) + \frac{\frac{A_3}{A_1}}{(3+(\frac{\Psi}{\ln(\frac{r_2}{r_1})})^2)^{\frac{1}{2}}})(\frac{\Psi}{\ln(\frac{r_2}{r_1})}) \quad (75)$$

4 RESULTS AND DISCUSSION

4.1. Results for the axial shear

For the axial shear, the boundary condition at the inner boundary is given by $f(R=R_1)=0$. At the outer boundary the axial displacement is denoted by d so that $f(R=R_2)=d$.

Thus for the Gent-Thomas, modified Gent-Thomas, and Gent-Gent materials, where the solution was reduced to quadrature, integration of "Eq. (27)", along with the two positive roots of "Eq. (39)", yields:

$$d = f(R=R_2) = \int_{R_1}^{R_2} f' \mathrm{d}R \quad (76)$$

To evaluate the above integral numerically, the fourth order Newton–Coats (Boole's rule) numerical integration technique [32] is used.

The Gent strain energy function is defined as [8]:

$$W_G = -\frac{\mu_1}{2} J_m \ln(1-\frac{I_1-3}{J_m}) \quad (77)$$

Where, μ_1 and J_m are the shear modulus and the limiting chain extensibility parameter, respectively.

Also, for the Gent model, the dimensionless axial shear displacement was determined to be [15]:

$$\frac{d}{r_1} = \frac{J_m\left((1-\eta^2)+\eta^2\sqrt{1+\frac{4T^2}{J_m}}-\sqrt{1+\frac{4\eta^2T^2}{J_m}}\right)}{4T\eta} + \eta T\ln\left[\frac{\eta\left(1+\sqrt{1+\frac{4T^2}{J_m}}\right)}{\left(1+\sqrt{1+\frac{4\eta^2T^2}{J_m}}\right)}\right] \quad (78)$$

Where, $T=T_1/\mu_1$ and $\eta=r_2/r_1$.

It is assumed that the cylindrical tube has the inner radius R_1=2 cm, the outer radius R_2 =4 cm with numerical values of K_1, K_2, $\mu/2$, C_2, A_1, A_2, and A_3, shown in "Tables 1, 2, and 3", respectively. For the modified Gent-Thomas strain energy, the value J_m=97.2 is considered based on the uniaxial experimental data reported by Gent [8].

The dimensionless axial shear traction for the Gent-Thomas and modified Gent-Thomas models is defined by $T=T_1/K_1$, and for the Gent-Gent and Carroll models is defined as $T=T_1/\mu$ and $T=T_1/A_1$, respectively.

In "Fig. 1", variations of the dimensionless axial displacement versus the dimensionless axial shear traction for the modified Gent-Thomas, Carroll, Gent-Gent, and Gent models are plotted.

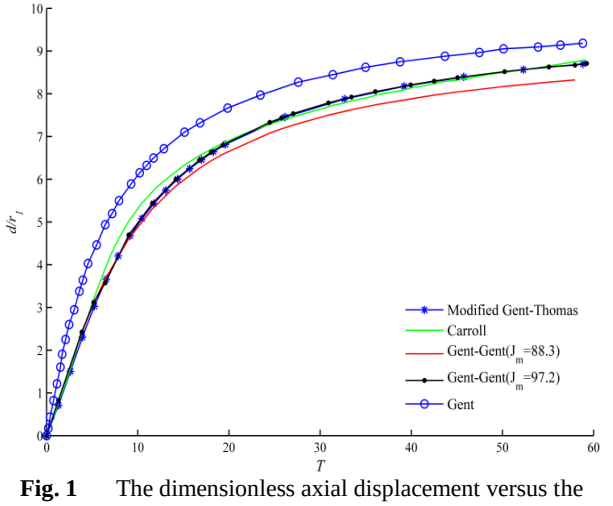

Fig. 1 The dimensionless axial displacement versus the dimensionless axial shear traction for the Modified Gent-Thomas, Carroll, Gent-Gent, and Gent models.

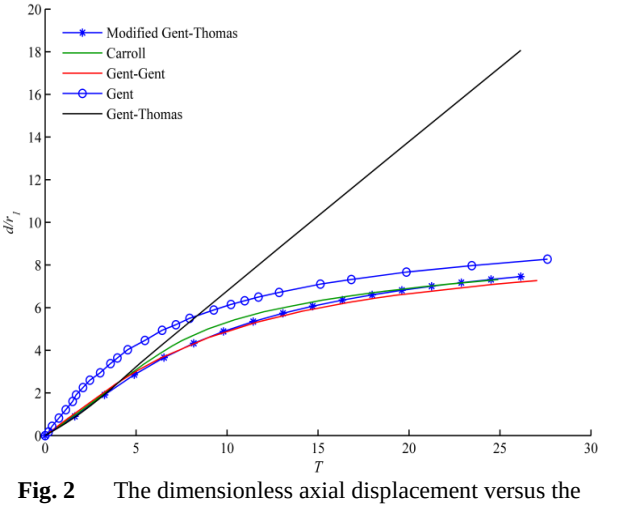

Fig. 2 The dimensionless axial displacement versus the dimensionless axial shear traction for the Modified Gent-Thomas, Carroll, Gent-Gent, Gent, and Gent-Thomas models.

The modified Gent-Thomas and Carroll models are shown to be in close agreement even though the former is microstructurally-based, while the latter is a phenomenological model. The close agreement between the two models is considered as an advantage for the modified Gent-Thomas model since the Carroll model shows considerable capability in predicting the behavior of rubber-like materials over a wide range of deformations.

The effect of the limiting chain extensibility condition is noticeable in the modified Gent-Thomas and Gent-Gent models. For J_m=97.2, both these models show very similar behavior in an axial shear deformation, and when this constant is reduced to J_m=88.3, the Gent-Gent model shows a higher resistance in the axial shear deformation indicating that the limiting chain extensibility parameter has a noticeable effect on the response of the material in such deformation.

Also, the Gent and the modified Gent-Thomas models differ only in the term involving the I_2 where it is absent in the former model and present in the latter. The two models have the same value of J_m=97.2. From "Fig. 1" it is clear that the modified Gent-Thomas model shows considerably more resistance in the axial shear deformation than the Gent model. This must be due to the presence of the second invariant of the deformation tensor I_2 in the modified Gent-Thomas model which has the effect of increasing the strain hardening experienced by the material in such deformation. In "Fig. 2", the effect of strain hardening for the modified Gent-Thomas, Carroll, Gent-Gent, and Gent models is shown to be quite pronounced for larger values of the axial shear traction, while the strain hardening effect is absent in the Gent-Thomas model due to the absence of the limiting chain extensibility parameter in this model.

4.2. Results for the azimuthal shear

For the azimuthal shear, the angle of twist for the Gent-Thomas, modified Gent-Thomas, and Carroll models can be determined using "Eqs. (66), (72), and (75)", respectively. For the azimuthal shear deformation, the shear stress for the Gent model, using "Eqs. (5), (55- 59), and (77)", is given by:

$$t_{r\theta} = 2\left(\frac{\frac{\mu_1}{2}}{1-\frac{\left(\frac{\Psi}{\ln(\frac{r_2}{r_1})}\right)^2}{J_m}}\right)\left(\frac{\Psi}{\ln(\frac{r_2}{r_1})}\right) \tag{79}$$

Therefore, the applied shear traction for this model is determined in terms of the angle of twist using "Eq. (79)" at the outer boundary as:

$$\bar{T} = \frac{1}{1-\frac{\left(\frac{\Psi}{\ln(\frac{r_2}{r_1})}\right)^2}{J_m}}\left(\frac{\Psi}{\ln(\frac{r_2}{r_1})}\right) \tag{80}$$

Where $\bar{T}=T_0/\mu_1$.

The angular displacement at the outer boundary, represented by the angle of twist, versus the dimensionless azimuthal shear traction for the above-mentioned models is plotted in "Fig. 3".

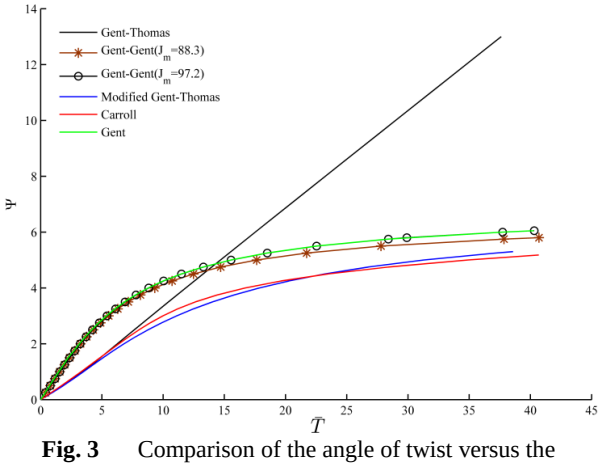

Fig. 3 Comparison of the angle of twist versus the dimensionless azimuthal shear traction for the modified Gent-Thomas, Gent-Gent, Carroll, and Gent models.

In "Fig. 3", the modified Gent-Thomas and Carroll models experience smaller angular displacement in azimuthal shear when subjected to the same shear traction in comparison to other models such as the Gent-Gent model. Therefore, they show higher resistance in azimuthal shear than the other models considered here. This is due to the fact that the coefficient multiplying the term involving I_2 in the Gent-Gent model, namely C_2= 0.0428 N/mm^2, is less than the third of the corresponding coefficient in the modified Gent-Thomas model, i.e., K_2= 0.147 N/mm^2. Thus, the effect of I_2 is to enhance the strain hardening of the material which causes the resistance of the modified Gent-Thomas model in azimuthal shear to increase.

The same can be inferred about the limiting chain extensibility parameter J_m, since when its value is changed from 97.2 to 88.3, making the polymeric chains more resistant to extension, the material shows more resistance in azimuthal shear deformation. Finally, for the same value of the limiting chain extensibility parameter, J_m =97.2, the Gent-Gent and Gent models have a very similar response in azimuthal shear deformation. This can be attributed to the small value of the coefficient multiplying the term involving I_2 in the Gent-Gent model, i.e., C_2= 0.0428 N/mm^2, causing the effect of I_2 to become so negligible as to render the response of this model nearly identical to a model with no dependence on I_2 such as the Gent model. As in the axial shear deformation, the Gent-Thomas model undergoes no strain hardening in azimuthal shear due to the absence of the limiting chain extensibility parameter.

5 CONCLUSION

In the present paper, axial and azimuthal shearing deformation of an incompressible hyperelastic solid with the modified Gent-Thomas, Gent-Thomas, Gent-Gent, and Carroll strain energy functions was considered. For an incompressible cylinder undergoing axial shear deformation, analytical solution for the modified Gent-Thomas, Gent-Gent and Gent-Thomas models, and numerical solution for the Carroll model were obtained and plotted in "Fig. 2". The last model which is a macroscopically-based model predicts the strain hardening effect at large elastic deformations which is also predicted by the modified Gent-Thomas model. In "Figs. 1 and 2", the modified Gent-Thomas and Carroll models were shown to be in close agreement even though the former is microstructurally-based while the latter is a phenomenological model.

The response of the modified Gent-Thomas model in axial shear was compared to that of the Gent model where the second invariant of the deformation I_2 is absent. It was concluded that for the same axial shear traction applied to the outer boundary, a cylinder with the modified Gent-Thomas model experiences less axial displacement than the one with the Gent model indicating that the second invariant increases the resistance of the material in axial shear deformation noticeably.

By comparing the response of the modified Gent-Thomas model with the Gent-Gent model, it was shown that the limiting chain extensibility parameter also enhances the resistance of the material in the axial shear deformation.

In addition, a controllable azimuthal shear deformation was considered and the angular displacement was obtained analytically for the modified Gent-Thomas, Gent-Thomas, Gent-Gent, and Carroll models with the results plotted in "Fig. 3". The response of the Gent model was also plotted in "Fig. 3". It can be concluded that the modified Gent-Thomas and Carroll models have a higher resistance in azimuthal shear deformation than the Gent-Gent model. This can be attributed to the second invariant of deformation tensor since the coefficient multiplying the term involving the second invariant in the modified Gent-Thomas model is almost three times as large as the corresponding coefficient in the Gent-Gent model. In addition, it was shown that for the same value of the limiting chain extensibility parameter, the Gent-Gent model and the Gent model have almost the same response in azimuthal shear due to the small coefficient multiplying the second invariant in the former model. It was also shown that the limiting chain extensibility parameter increases the resistance of the material in the azimuthal shear deformation.

In conclusion, it can be stated that when a polymeric material with one of the strain energy models considered above undergoes a nonhomogeneous shearing deformation such as an axial or azimuthal shear, the effect of the second invariant of the deformation tensor is to increase the strain hardening experienced by the material. This increase in the strain hardening due to the presence of the second invariant, which has not been studied in detail before, causes the material to become more resistant and therefore, to undergo less deformation under the same type of loading. The same can be stated for the limiting chain extensibility parameter whenever it is present in the model, such as in the modified Gent-Thomas and Gent-Gent models.

APPENDIX

In this Appendix, the four roots of "Eq. (39)" are reported as:

$$f' = -\frac{r}{4bT} - \frac{1}{2}\sqrt{X - \frac{0.4196Q}{bTS} - \frac{S}{3.7797bT}} - \frac{1}{2}\sqrt{X + \frac{0.4196Q}{bTS} + \frac{S}{3.7797bT} - E} \quad \text{(A1)}$$

$$f' = -\frac{r}{4bT} - \frac{1}{2}\sqrt{X - \frac{0.4196Q}{bTS} - \frac{S}{3.7797bT}} + \frac{1}{2}\sqrt{X + \frac{0.4196Q}{bTS} + \frac{S}{3.7797bT} - E} \quad \text{(A2)}$$

$$f' = -\frac{r}{4bT} + \frac{1}{2}\sqrt{X - \frac{0.4196Q}{bTS} - \frac{S}{3.7797bT}} - \frac{1}{2}\sqrt{X + \frac{0.4196Q}{bTS} + \frac{S}{3.7797bT} + E} \quad \text{(A3)}$$

$$f' = -\frac{r}{4bT} + \frac{1}{2}\sqrt{X - \frac{0.4196Q}{bTS} - \frac{S}{3.7797bT}} + \frac{1}{2}\sqrt{X + \frac{0.4196Q}{bTS} + \frac{S}{3.7797bT} + E} \quad \text{(A4)}$$

Where:

$$E = \frac{Y}{4\sqrt{X - \frac{0.4196Q}{bTS} - \frac{S}{3.7797bT}}} \quad \text{(A5)}$$

$$S = (L + \sqrt{-4Q^3 + L^2})^{\frac{1}{3}} \quad \text{(A6)}$$

$$\begin{aligned} L &= -27b\,J_m\,r^2T\,(J_mK_m^2 - 3) \\ &+ bT\,(J_m - 3)(2b^2T^2((J_m - 3)^2 + 108J_m) - 9J_mK_mr^2) \end{aligned} \quad \text{(A7)}$$

$$Q = b^2T^2((J_m - 3)^2 - 36J_m) - 3r^2J_mK_m \quad \text{(A8)}$$

$$X = \frac{2}{3}(J_m - 3) + \frac{r^2}{4b^2T^2} \quad \text{(A9)}$$

$$Y = (\frac{r}{bT})(4(3 - J_m) - 8J_mK_m - (\frac{r}{bT})^2) \quad \text{(A10)}$$

Equations (A1) and (A3) above have negative signs. Therefore, to ensure that $f'(R)>0$, only "Eqs. (A2) and (A4)" are considered which are the second and the fourth roots of "Eq. (39)", respectively. Equations (A2) and (A4) are used to plot the angle of twist versus the dimensionless azimuthal shear traction.

REFERENCES

[1] Hayes, M., Saccomandi, G., Topics in Finite Elasticity, Springer-Verlag, New York, USA, 2001, pp. 31-93, ISBN: 978-3-211-83336-0.

[2] Gent, A. N., Elastic Instabilities in Rubber, International Journal of Non-Linear Mechanics, Vol. 40, No. 2-3, 2005, pp. 165-175, DOI: 10.1016/j.ijnonlinmec.2004.05.006.

[3] Warne, D. A., Warne, P. G., Torsion in Nonlinearly Elastic Incompressible Circular Cylinders, International Journal of Non-Linear Mechanics, Vol. 86, 2016, pp. 158-166, DOI: 10.1016/j.ijnonlinmec.2016.08.008.

[4] Gent, A. N., Thomas, A. G., Forms for the Stored (Strain) Energy Function for Vulcanized Rubber, Journal of Polymer Science, Vol. 28, No. 118, 1958, pp. 625–628, DOI: 10.1002/pol.1958.1202811814.

[5] Pucci, E., Saccomandi, G., A Note on the Gent Model for Rubber-Like Materials, Rubber Chemistry and Technology, Vol. 75, No. 5, 2002, pp. 839-852, DOI: 10.5254/1.3547687.

[6] Carroll, M. M., A Strain Energy Function for Vulcanized Rubbers, Journal of Elasticity, Vol. 103, No. 2, 2011, pp. 173-187, DOI: 10.1007/s10659-010-9279-0.

[7] Gent, A. N., Extensibility of Rubber under Different Types of Deformation, Journal of Rheology, Vol. 49, No. 1, 2005, pp. 271-275, DOI: 10.1122/1.1835343.

[8] Gent A. N., 1996, A New Constitutive Relation for Rubber, Rubber Chemistry and Technology, Vol. 69, No. 1, 1996, pp. 59-61, DOI: 10.5254/1.3538357.

[9] Kilian, H. G., Equation of State of Real Networks, Polymer, Vol. 22, No. 2, 1981, pp. 209–217, DOI: 10.1016/0032-3861(81)90200-7.

[10] Edwards, S. F., Vilgis, T., The Effect of Entanglements in Rubber Elasticity, Polymer, Vol. 27, No. 4, 1986, pp. 483–492, DOI: 10.1016/0032-3861(86)90231-4.

[11] Zidi, M., Combined Torsion, Circular and Axial Shearing of a Compressible Hyperelastic and Prestressed, Journal of Applied Mechanics, Vol. 67, No. 1, 2000, pp. 33-40, DOI: 10.1115/1.321149.

[12] Ogden, R.W., Chadwick, P., and Haddon, E. W., Combined Axial and Torsional Shear of a Tube of Incompressible Isotropic Elastic Material, The Quarterly Journal of Mechanics and Applied Mathematics, Vol. 26, No. 1, 1973, pp. 23-41, DOI: 10.1093/qjmam/26.1.23.

[13] Jiang, X., Ogden, R. W., Some New Solutions for the Axial Shear of a Circular Cylindrical Tube of Compressible Elastic Material, International Journal of Non-linear Mechanics, Vol. 35, No. 2, 2000, pp. 361-369, DOI: 10.1016/S0020-7462(99)00041-4.

[14] Kanner, L. M., Horgan, C. O., Inhomogeneous Shearing of Strain Stiffening Rubber-Like Hollow Circular Cylinders, International Journal of Solids and Structures, Vol. 45, No. 20, 2008, pp. 5464-5482, DOI: 10.1016/j.ijsolstr.2008.05.030.

[15] Horgan, C. O., Saccomandi, G., Pure Axial Shear of Isotropic, Incompressible Nonlinearly Elastic Materials With Limiting Chain Extensibility, Journal of Elasticity Vol. 57, No. 3, 1999, pp. 307-319, DOI:10.1023/A:1007639129264.

[16] Benjamin, C. C., Myneni, M., Muliana, A., and Rajagopal, K. R., Motion of a Finite Composite Cylindrical Annulus Comprised of Nonlinear Elastic Solids Subject to Periodic Shear, International Journal of Non-Linear Mechanics, Vol. 113, 2019, pp. 31-43, DOI: 10.1016/j.ijnonlinmec.2019.03.010.

[17] Horgan, C. O., Saccomandi, G., and Sgura, I., A Two-Point Boundary-Value Problem for the Axial Shear of Hardening Isotropic Incompressible Nonlinearly Elastic Materials, SIAM Journal on Applied Mathematics, Vol. 62, No. 5, 2002, pp. 1712-1727, DOI: 10.1137/S0036139901391963.

[18] Steinmann, P., Hossain, M., and Possart, G., Hyperelastic Models for Rubber-Like Materials: Consistent Tangent Operators and Suitability for Treloar's Data, Archive of Applied Mechanics, Vol. 82, No. 9, 2012, pp. 1183-1217, DOI: 10.1007/s00419-012-0610-z.

[19] Destrade, M., Saccomandi, G., and Sgura, I., Methodical Fitting for Mathematical Models of Rubber-Like Materials, Proceedings of the Royal Society A: Mathematical, Physical and Engineering Sciences, Vol. 473, No. 2198, 2017, pp. 20160811, DOI: 10.1098/rspa.2016.0811.

[20] Zidi, M., Azimuthal Shearing and Torsion of a Compressible Hyperelastic and Prestressed Tube, International Journal of Non-Linear Mechanics, Vol. 3, No. 2, 2000, pp. 201-209, DOI: 10.1016/S0020-7462(99)00008-6.

[21] Zidi, M., Large Shearing of a Prestressed Tube, Journal of Applied Mechanics, Vol. 67, No. 1, 2000, pp. 1-4, DOI:10.1115/1.321175.

[22] Horgan, C. O., Saccomandi, G., Pure Azimuthal Shear of Isotropic, Incompressible Hyperelastic Materials with Limiting Chain Extensibility, International Journal of Non-Linear Mechanics, Vol. 3, No. 3, 2001, pp. 465-475, DOI: 10.1016/S0020-7462(00)00048-2.

[23] Dagher, M. A., Soldatos, K. P., Pure Azimuthal Shear Deformation of an Incompressible Tube Reinforced by Radial Fibres Resistant in Bending, The IMA Journal of Applied Mathematics, Vol. 79, No. 5, 2014, pp. 848–868, DOI: 10.1093/imamat/hxu013.

[24] Bustamante, R., Some Universal Solutions for a Class of Incompressible Elastic Body that is not Green Elastic: The Case of Large Elastic Deformations, The Quarterly Journal of Mechanics and Applied Mathematics, Vol. 73, No. 2, 2020, pp. 177-199, DOI: 10.1093/qjmam/hbaa006.

[25] El Hamdaoui, M., Merodio, J., and Ogden, R. W., Deformation Induced Loss of Ellipticity in an Anisotropic Circular Cylindrical Tube, Journal of Engineering Mathematics, Vol. 109, No. 1, 2018, pp. 31-45, DOI: 10.1007/s10665-017-9904-z.

[26] Horgan, C. O., Saccomandi, G., Helical Shear for Hardening Generalized Neo-Hookean Elastic Materials, Mathematics and Mechanics of Solids, Vol. 8, No. 5, 2003, pp. 539-559, DOI: 10.1177/10812865030085007.

[27] Anssari-Benam, A., Bucchi, A., A Generalised Neo-Hookean Strain Energy Function for Application to The Finite Deformation of Elastomers, International Journal of Non-Linear Mechanics, Vol. 128, 2021, pp. 103626, DOI: 10.1016/j.ijnonlinmec.2020.103626.

[28] Ghafouri Sayyad, A., Imam, A., and Etemadi Haghighi, S., Evaluating the Response of a Modified Gent-Thomas Strain Energy Function Having Limiting Chain Extensibility Condition in Torsion and Azimuthal Shear, Polymers and Polymer Composites, 2021, DOI: 10.1177/09673911211003394.

[29] Marckmann, G., Verron, E., Comparison of Hyperelastic Models for Rubber-Like Materials, Rubber Chemistry and Technology, Vol. 79, No. 5, 2006, pp. 835-858, DOI: DOI:10.5254/1.3547969.

[30] Ogden, R. W., Non-Linear Elastic Deformations, Ellis Horwood, Chichester, England, 1984, pp. 224-326, ISBN: 0-8-5312-273-3.

[31] Ogden, R.W., Saccomandi, G., and Sgura, I., Fitting Hyperelastic Models to Experimental Data, Computational Mechanic, Vol. 34, No. 6, 2004, pp. 484-502, DOI: 10.1007/s00466-004-0593-y.

[32] Abramowitz, M., Stegun I. A., Handbook of Mathematical Functions: With Formulas, Graphs, and Mathematical Tables, Dover, New York, USA, 1965, pp. 885-887, ISBN: 978-0486612720.